



Published in final edited form as:

Radiology. 2002 January ; 222(1): 212–218.

Correlation of White Matter Diffusivity and Anisotropy with Age during Childhood and Adolescence: A Cross-sectional Diffusion-Tensor MR Imaging Study

Vincent J. Schmithorst, PhD, Marko Wilke, MD, Bernard J. Dardzinski, PhD, and Scott K. Holland, PhD

From the Imaging Research Center, Children's Hospital Medical Center, 3333 Burnet Ave, Suite R050A, Cincinnati, OH 45229

Abstract

PURPOSE—To evaluate differences in white matter diffusion properties as a function of age in healthy children and adolescents.

MATERIALS AND METHODS—Echo-planar diffusion-tensor magnetic resonance (MR) imaging was performed in 33 healthy subjects aged 5–18 years who were recruited from a functional imaging study of normal language development. Results of neurologic, psychologic, and structural MR imaging examinations were within the normal range for all subjects. The trace of the apparent diffusion coefficient and fractional anisotropy in white matter were correlated as a function of age by using Spearman rank correlation.

RESULTS—Statistically significant negative correlation of the trace of the apparent diffusion coefficient with age was found throughout the white matter. Significant positive correlation of fractional anisotropy with age was found in the internal capsule, corticospinal tract, left arcuate fasciculus, and right inferior longitudinal fasciculus.

CONCLUSION—Diffusion-tensor MR imaging results indicate that white matter maturation assessed at different ages involves increases in both white matter density and organization during childhood and adolescence. The trace of the apparent diffusion coefficient and fractional anisotropy may reflect different physiologic processes in healthy children and adolescents.

Index terms

Anisotropy; Brain, diffusion, 10.12144; Brain, growth and development, 10.92; Brain, MR, 10.121411, 10.12144; Brain, white matter, 10.92; Children, central nervous system; Diffusion tensor; Magnetic resonance (MR), diffusion study, 10.12144, 10.92; Myelin, 10.92

Although most of the myelination in brain white matter is complete by the age of 5 years (1), maturation of brain white matter is an ongoing process into at least the 3rd decade of life (2–5). This maturation of brain structures and their connecting pathways is essential for the continuing development of both cognitive and motor functions, as the speed of neural transmission depends on the axon diameter and the thickness of the insulating myelin sheath (6). Results of previous postmortem analysis have shown that axon diameter and myelin sheath

Address correspondence to V.J.S. (e-mail: vince@athena.chmcc.org).

Author contributions

Guarantors of integrity of entire study, B.J.D., S.K.H., V.J.S.; study concepts and design, B.J.D., S.K.H.; literature research, M.W.; experimental studies, V.J.S.; data acquisition, V.J.S.; data analysis/interpretation, M.W., B.J.D., V.J.S.; statistical analysis, V.J.S.; manuscript preparation, B.J.D., V.J.S.; manuscript definition of intellectual content, S.K.H.; manuscript editing, M.W., B.J.D., S.K.H.; manuscript revision/review and final version approval, all authors.

grow markedly from birth until about the age of 2 years (7) and that these maturation processes may continue during adolescence and adulthood (8). However, little postmortem analysis information is available for childhood and adolescence. Thus, it is difficult to draw definite conclusions about the development of white matter in this age group.

Diffusion-tensor magnetic resonance (MR) imaging can be used to investigate and visualize the microscopic diffusion properties of water in living tissue. White matter fiber orientation can be determined by using diffusion-tensor MR imaging because water diffuses faster parallel to the longitudinal axis of axons than it does perpendicular to it (9,10). Therefore, among the in vivo MR imaging techniques, diffusion-tensor MR imaging in particular is an extremely useful tool for looking at white matter maturation during childhood (11).

Results of previous diffusion-tensor MR imaging studies show an increase in diffusion anisotropy in the posterior limb of the internal capsule and the central white matter in newborns (12), as well as a steady decrease in white matter anisotropy after 20 years of age (13). However, there is a lack of data regarding changes in the trace of the diffusion tensor or fractional anisotropy in different regions of the brain during infancy and childhood (14). The purpose of our study was to evaluate differences in white matter diffusion properties as a function of age in healthy children and adolescents.

MATERIALS AND METHODS

Subject Selection

Subjects were recruited as part of an ongoing functional MR imaging study of normal language development (15). Institutional review board approval and informed consent were obtained for all subjects. Exclusion criteria were previous neurologic illness, learning disability, head trauma with loss of consciousness, current or past use of psychostimulant medication, pregnancy, IQ less than 80 (measured by means of the Wechsler Intelligence Scale for Children, third edition), birth at gestational age of 37 weeks or fewer, or abnormal findings at routine neurologic examination. Thirty-three healthy subjects (16 male subjects, 17 female subjects; age range, 5–18 years; mean age, 10.8 years \pm 3.7 [SD]) who underwent imaging between July and November 2000 were included in this study after exclusion of contraindications. The Table provides data about the number of subjects according to age and sex. All but two subjects were right handed.

Imaging Parameters

Subjects underwent MR imaging with a 3-T imager (Biospec 30/60; Bruker Medical, Karlsruhe, Germany) equipped with a head gradient insert (± 45 mT/m). Diffusion-weighted spin-echo single-shot echo-planar MR imaging included the following parameters: repetition time msec/echo time msec, 3,250/80; matrix, 64×128 ; field of view, 19.2×25.6 cm; section thickness, 5 mm; readout bandwidth, 125 kHz; Δ , 40 msec; δ , 15 msec. Sixteen sections centered around the corpus callosum were acquired.

Two b values (diffusion-weighting factors), 814 and 994 sec/mm², were used with six gradient directions of [1,0,0], [0,1,0], [0,0,1], [$1/\sqrt{2}, 1/\sqrt{2}, 0/\sqrt{2}$], [$1/\sqrt{2}, 0/\sqrt{2}, 1/\sqrt{2}$], and [$0/\sqrt{2}, 1/\sqrt{2}, 1/\sqrt{2}$], where the numbers within brackets refer to the x, y, and z axes, respectively. An additional image was acquired with no diffusion weighting ($b = 0$ sec/mm²). The use of six gradient directions adequately characterizes the full diffusion tensor (16). For each b value and gradient direction, two images were acquired, and magnitude averaging was used to avoid artifacts from subject motion. The total imaging time for the entire diffusion-tensor MR imaging sequence was 90 seconds. In addition, a structural whole-brain T1-weighted modified driven-equilibrium

Fourier transform image (17) was acquired for anatomic coregistration. A qualified pediatric neuroradiologist read all MR images for structural abnormalities.

Image Processing and Analysis

The geometric distortion in the diffusion-weighted echo-planar MR images because of eddy currents was corrected with an iterative least squares algorithm. Since the presence of cerebrospinal fluid in the image with no diffusion weighting ($b = 0 \text{ sec/mm}^2$) may lead to excessive stretching in the diffusion-weighted MR images (18), the absolute value of the images filtered with a Sobel edge-enhancement filter was used to find the optimum values of shear, stretch, and shift. The first diffusion-weighted MR image in the sequence was spatially transformed to the image with no diffusion weighting ($b = 0 \text{ sec/mm}^2$) by means of minimizing the sum of the squares of the difference of the edge-enhanced diffusion-weighted MR image from the image with no diffusion weighting ($b = 0 \text{ sec/mm}^2$) by using a conventional Levenberg-Marquardt algorithm. The subsequent diffusion-weighted MR images were then spatially transformed to the first one in the same manner.

The distortion due to the static magnetic field inhomogeneities present in the image with no diffusion weighting ($b = 0 \text{ sec/mm}^2$) was corrected by means of a multiecho reference image (19,20). The echo-planar images were then transformed into stereotactic, or Talairach, space. To increase the signal-to-noise ratio, the images were filtered by using a Gaussian kernel with a full width at half maximum of 3 mm prior to the transformation. The whole-brain data sets were also transformed into Talairach space and averaged for all subjects. By using a k-means clustering algorithm, a white matter template based on the averaged brain values was applied to exclude cortical gray matter and cerebrospinal fluid to avoid partial-volume effects (21) in the diffusion-tensor MR imaging data processing that followed.

For each data set, the diffusion-tensor matrix eigenvectors, eigenvalues, trace of the apparent diffusion coefficient, and fractional anisotropy were calculated for the white matter covered by the image. Fractional anisotropy is a robust estimator of diffusion anisotropy (22) and is rotationally invariant (ie, independent of the actual fiber direction and the hardware used) (23).

On a pixel-by-pixel basis, the trace of the apparent diffusion coefficient and fractional anisotropy values calculated from the filtered images were correlated with subject age, in days at date of examination, by using the Spearman rank correlation test. Pixels for which the P value was less than .05 were then assigned a color value according to the correlation coefficient and overlaid on top of the averaged ($n = 33$) whole-brain structural MR images. To increase the statistical power (24), the colored pixels were clustered in three dimensions with a cluster size of 15. To illustrate the relationship between absolute values and age while avoiding the inconsistency of hand-drawn regions of interest, the values of age-correlated pixels in one complete section were correlated with the corresponding measures—trace of the apparent diffusion coefficient and fractional anisotropy.

RESULTS

The neuroradiologist read all whole-brain images as normal. Results of neurologic and psychologic examinations were all within normal limits for the subjects' ages.

The statistical parameter map showing areas of significant negative correlation of the trace of the apparent diffusion coefficient with age is shown in Figure 1. Changes are found throughout the white matter in a roughly symmetric pattern. Small areas of significant positive correlation were seen only in low fronto-orbital regions and close to the lateral ventricles on both sides.

The map that demonstrates areas of significant positive correlation of fractional anisotropy with age is shown in Figure 2. These areas involved the internal capsule, corticospinal tract, left arcuate fasciculus, and right inferior longitudinal fasciculus. Significant negative correlation was detected bilaterally in two small clusters next to the frontal horn of the lateral ventricles and adjacent to the caudate nucleus. Figure 3 shows the trace of the apparent diffusion coefficient as a function of subject age for the significantly correlated pixels in the sixth section in Figure 1, which is depicted in the second image from left in the middle row, and Figure 4 shows fractional anisotropy as a function of subject age for the significantly correlated pixels in the sixth section (second image from left in the middle row) of Figure 2.

DISCUSSION

Subjects and Methods

We investigated a sample of healthy male and female subjects 5–18 years old. In contrast to the subjects in earlier studies, the subjects in our study were healthy and were specifically recruited for the investigation of normal brain development. Therefore, we consider our data reliable and representative of a healthy population and are able to avoid the potential problem of lack of transferability of results (25).

Lower Values in the Trace of the Apparent Diffusion Coefficient with Age

Areas in which the trace of the apparent diffusion coefficient negatively correlated with subject age were found throughout the white matter (Fig 1). Although white matter values for the trace of the apparent diffusion coefficient approach adult values within the 1st year of life (26), we were able to demonstrate ongoing changes with age in specific regions of brain white matter.

The changes in the values for the trace of the apparent diffusion coefficient involve mainly association and commissural fibers, which connect different areas of the cortex with each other. This hints at an ongoing process of modification in these fiber tracts, which has been observed in association cortex in postmortem studies (5). This refinement is more pronounced in children than in adults (27). The fact that there is no accompanying increase in fractional anisotropy might be explained by the observation that anisotropy is small in white matter regions with changing fiber direction (16,28). The many small developing and maturing association fibers connecting different cortical areas with each other and with subcortical structures may not lead to a concomitant increase in the degree of organization, which therefore gives rise to changes in the trace of the apparent diffusion coefficient but not to changes in fractional anisotropy.

Higher Values in Fractional Anisotropy with Age

As did the subjects in previous studies (11,12,16,29), the subjects in our study displayed the highest values of fractional anisotropy in the internal capsule. The correlation with subject age was also strongest in the internal capsule and the corresponding projective fiber tracts descending to or ascending from it. These correspond to corticospinal, corticonuclear, and possibly thalamocortical tracts (30). The correlation seems to be most pronounced in fibers passing to primary and supplementary motor areas (Brodmann areas 4 and 6), which is consistent with ongoing maturation and refinement of fine motor control, especially finger movements (30).

The correlation in the internal capsule seems to overlap with the neighboring basal ganglia structures, especially the globus pallidus, which also shows a decrease in values for the trace of the apparent diffusion coefficient with age. This overlap has been seen before in structural analyses (30), as well as in diffusion data analyses (31), and might exist for several reasons: true anatomic overlap (31), actual anisotropy increases within the basal ganglia (11,31), or volume decreases with age (32). Theoretically, iron deposition in older children (33) could

lead to false results. Spatial normalization could also influence results, as the brains of younger children might have to undergo stronger spatial transformations (34).

A statistically significant correlation of increased fractional anisotropy with age was found in only two other distinct white matter regions, namely the right inferior longitudinal fasciculus and the left arcuate fasciculus. The inferior longitudinal fasciculus consists of long fiber tracts connecting parietal and temporal areas. Especially in the dorsal aspects, a partial overlap is seen with the decrease in the trace of the apparent diffusion coefficient.

The arcuate fasciculus showed a significant increase in fractional anisotropy on only the left side. This is an intriguing finding because of the function of these fibers in the interaction of the two major language areas, which are traditionally known as the Broca and Wernicke areas. Because both language capabilities and hemispheric lateralization strongly increase during childhood, our findings could lend support to the hypothesis that the structural changes in the brain that occur during postnatal development should correlate with location and amount of regional brain activation (25,35). This would imply a continued refinement and strengthening of these connections, which is compatible with the ongoing refinement of language function during normal development. At present, it is unclear which process distinguishes these two fiber tracts. Either a substantially different organization of fibers or a markedly longer duration of the maturational processes could lead to their detection in our analysis, but at present, there are not enough data to support either of these hypotheses.

Pathophysiologic Considerations

The widespread changes in the trace of the apparent diffusion coefficient are not easily explained by newly formed myelin, as suggested before (36), because myelination is essentially complete by the age of 5 years (1), and there is no further marked increase in cerebral volume (4). Also, myelin would also be expected to increase in the internal capsule, where we see highly significant changes in fractional anisotropy but not in values for the trace of the apparent diffusion coefficient. Therefore, we suggest that myelination status in children after infancy is not adequately reflected in the trace of the apparent diffusion coefficient alone. However, it may reflect white matter maturation more closely than do anisotropy measurements in fiber tracts without a high degree of organization.

Increases in anisotropy in white matter are traditionally believed to reflect increasing myelination (11), because of the assumption that water movement is more restricted perpendicular to myelin membranes than it is parallel to them (14). Significant anisotropy within the human brain is present without detectable myelin (37), and results of in vitro experiments show that the difference in anisotropy between myelinated and un-myelinated fibers is surprisingly small (38). This finding led to the conclusion that anisotropy of water diffusion cannot be expected to be a specific marker of myelination in white matter (38).

Therefore, anisotropy seems to reflect influences from cellular components, such as cellular membranes (14), as well as from the local microstructural texture (31,39). These influences might include tissue hydration, myelination, cell-packing density and fiber diameter, and directional coherence (14,31,39). Because the water content of the brain reaches a steady level by the age of 1 year (40,41), and global myelination detectable by means of conventional MR imaging is essentially complete by the age of 5 years (1), we do not believe the changes in fractional anisotropy in our study were caused by either of these two factors.

Fiber diameter and cell-packing density should not be considered separately: Axons with a larger diameter also have a thicker myelin sheath (42), and myelinated axons take up considerably more space than do nonmyelinated axons (14). Axon diameter in central motor and sensory pathways is known to increase with the height of the individual (43) to ensure

constant central conduction times, and the corticospinal motor pathway continues to mature electrophysiologically until the age of at least 13 years (44). Depending on their final maximum diameter (45), axons are myelinated by different subtypes of oligodendrocytes, so the local microstructure might furthermore reflect not only neuronal but also glial cell differences.

Axons in the projective, primarily corticospinal, tracts are tightly packed and highly organized when funneled through the internal capsule (30). Over time, their increase in diameter and myelin sheath would require an increasing degree of structural organization because of the restricted space available. This higher degree of fiber tract organization has been shown before to lead to an increase in fractional anisotropy but not in the trace of the apparent diffusion coefficient during nerve development (46), which is brought about by an increase in longitudinal diffusion without a concomitant decrease in transverse diffusion. This process would explain the increasingly anisotropic diffusion with age seen in our study.

Changes in the internal capsule, the corticospinal tract, and the arcuate fasciculus that we observed strikingly resemble recent findings (30) of age-related increases in white matter density detected by means of conventional MR imaging. This increasing white matter density seems to correlate closely with the increase we see in fractional anisotropy. Therefore, the further increase in organization of the already highly parallel fibers in the descending pathways, which leads to an increase in fractional anisotropy, seems to yield a substantially more dense tissue microstructure detected by means of an increase in signal intensity on conventional T1-weighted MR images but not in values for the trace of the apparent diffusion coefficient. It was suggested before that differences in fractional anisotropy might reflect different histologic properties of white matter (31), and our results seem to lend support to this hypothesis.

The minimal overlap in decreases in the trace of the apparent diffusion coefficient and increases in fractional anisotropy may indicate that they mainly reflect different physiologic processes. On the basis of data in animals, it was suggested that changes in the trace of the apparent diffusion coefficient with maturation primarily are caused by changes in the intracellular compartment that are brought about by a greater membrane surface-to-cell volume ratio and a greater concentration of membranes (23). This proposed mechanism in development is different from the changes in the trace of the apparent diffusion coefficient in acute tissue ischemia, which correlate with the extracellular volume fraction (47).

In contrast to the decreases in the trace of the apparent diffusion coefficient, the age-related increases in fractional anisotropy in our study would be compatible with a mechanism of an increasingly dense and ordered packing of fiber tracts as seen before in nerve maturation (46), which leads to a directionally more restricted extracellular, rather than intra-cellular, space. Also, the strong resemblance with the white matter density changes found by means of conventional imaging (30) suggests that only this process, which leads to an increase in fractional anisotropy but not in the trace of the apparent diffusion coefficient, is accompanied by changes in T1. However, although our data would be compatible with such an explanation, further research about these issues is necessary.

Limitations of This Study

Although we were able to show statistically significant correlations with age for both the trace of the apparent diffusion coefficient and fractional anisotropy in distinct areas, our study is nevertheless limited by several factors. The relatively low 2×3 -mm in-plane resolution and 5-mm section thickness may result in smaller fiber tracts not being seen. Also, because of hardware limitations, we were able to acquire only 16 sections; thus, the whole brain was not covered. Spatial normalization, although shown to be fairly reliable in another study (34) involving subjects in the same age range as those in our study, is nevertheless not as robust as

it is in adult brains, and this could lead to some partial-volume overlap between white matter and adjacent structures.

Since only 33 subjects participated in the study, there were relatively few subjects per age. There was only one subject for ages 5, 6, 12, 13, and 14 years, and there were no subjects at all for age 16 years. Although not a limitation per se, we wish to emphasize that our data were obtained from different subjects of different ages, rather than from the same subjects as they aged over time. With only 33 children, it is questionable to attempt to fit a higher order model to our data by using nonlinear regression. It is evident with our data that linear regression is probably not the best model for the developmental patterns seen in the trace of the apparent diffusion coefficient and fractional anisotropy, as one might expect these changes to correlate with the temporal variation of brain development.

In conclusion, we have shown statistically significant decreases in the trace of the apparent diffusion coefficient and increases in fractional anisotropy with age in a group of healthy children and adolescents, and we suggest that these two findings may reflect two different underlying physiologic processes. Decreases in values for the trace of the apparent diffusion coefficient suggest that these reflect increases in white matter structure without a concomitant increase in organization, which is induced by ongoing maturation in primarily cortical association fibers. In the more regionally specific increases in fractional anisotropy, we attribute this to the higher degree of organization and possibly the changing microstructural characteristics of primarily projective axons. Increasing organization in the left arcuate fasciculus is consistent with previous findings of increasing left lateralization of semantic language areas with age, as shown by means of functional MR imaging (35).

Acknowledgements

Supported by grant RO1 HD38578-02 from the National Institute of Child Health and Human Development.

References

1. Nakagawa H, Iwasaki S, Kichikawa K, et al. Normal myelination of anatomic nerve fiber bundles: MR analysis. *AJNR Am J Neuroradiol* 1998;19:1129–1136. [PubMed: 9672026]
2. Pfefferbaum A, Mathalon DH, Sullivan EV, Rawles JM, Zipursky RB, Lim KO. A quantitative magnetic resonance imaging study of changes in brain morphology from infancy to late adulthood. *Arch Neurol* 1994;51:874–887. [PubMed: 8080387]
3. Courchesne E, Chisum HJ, Townsend J, et al. Normal brain development and aging: quantitative analysis at in vivo MR imaging in healthy volunteers. *Radiology* 2000;216:672–682. [PubMed: 10966694]
4. Casey BJ, Giedd JN, Thomas KM. Structural and functional brain development and its relation to cognitive development. *Biol Psychol* 2000;54:241–257. [PubMed: 11035225]
5. Huttenlocher PR, Dabholkar AS. Regional differences in synaptogenesis in human cerebral cortex. *J Comp Neurol* 1997;387:167–178. [PubMed: 9336221]
6. Aboitiz F, Scheibel AB, Fisher RS, Zaidel E. Fiber composition of the human corpus callosum. *Brain Res* 1992;598:143–153. [PubMed: 1486477]
7. Brody BA, Kinney HC, Kloman AS, Gilles FH. Sequence of central nervous system myelination in human infancy. I. An autopsy study of myelination. *J Neuropathol Exp Neurol* 1987;46:283–301. [PubMed: 3559630]
8. Benes FM, Turtle M, Khan Y, Farol P. Myelination of a key relay zone in the hippocampal formation occurs in the human brain during childhood, adolescence, and adulthood. *Arch Gen Psychiatry* 1994;51:477–484. [PubMed: 8192550]
9. Le Bihan, DL.; Turner, R.; Patronas, N. Diffusion MR imaging in normal brain and in brain tumors. In: Le Bihan, DL., editor. *Diffusion and perfusion magnetic resonance imaging: applications to functional MRI*. New York, NY: Raven; 1995. p. 134-140.

10. Peled S, Gudbjartsson H, Westin CF, Kikinis R, Jolesz FA. Magnetic resonance imaging shows orientation and asymmetry of white matter fiber tracts. *Brain Res* 1998;780:27–33. [PubMed: 9473573]
11. Morriss MC, Zimmerman RA, Bilaniuk LT, Hunter JV, Haselgrove JC. Changes in brain water diffusion during childhood. *Neuroradiology* 1999;41:929–934. [PubMed: 10639670]
12. Huppi PS, Maier SE, Peled S, et al. Microstructural development of human newborn cerebral white matter assessed in vivo by diffusion tensor magnetic resonance imaging. *Pediatr Res* 1998;44:584–590. [PubMed: 9773850]
13. Pfefferbaum A, Sullivan EV, Hedehus M, Lim KO, Adalsteinsson E, Moseley M. Age-related decline in brain white matter anisotropy measured with spatially corrected echo-planar diffusion tensor imaging. *Magn Reson Med* 2000;44:259–268. [PubMed: 10918325]
14. Barkovich AJ. Concepts of myelin and myelination in neuroradiology. *AJNR Am J Neuroradiol* 2000;21:1099–1109. [PubMed: 10871022]
15. Holland, SK. Proceedings of the Seventh Annual Meeting of the Organization for Human Brain Mapping. Brighton, England: Organization for Human Brain Mapping; 2001. Functional magnetic resonance imaging of normal language development (abstr); p. 542
16. Basser PJ, Pierpaoli C. Microstructural and physiological features of tissues elucidated by quantitative-diffusion-tensor MRI. *J Magn Reson B* 1996;111:209–219. [PubMed: 8661285]
17. Ugurbil K, Garwood M, Ellermann J, et al. Imaging at high magnetic fields: initial experiences at 4 T. *Magn Reson Q* 1993;9:259–277. [PubMed: 8274375]
18. de Crespigny, A.; Moseley, M. Proceedings of the Sixth Meeting of the International Society for Magnetic Resonance in Medicine. Berkeley, Calif: International Society for Magnetic Resonance in Medicine; 1998. Eddy current induced image warping in diffusion weighted EPI (abstr); p. 661
19. Chen NK, Wyrwicz AM. Correction for EPI distortions using multi-echo gradient-echo imaging. *Magn Reson Med* 1999;41:1206–1213. [PubMed: 10371453]
20. Schmithorst VJ, Dardzinski BJ, Holland SK. Simultaneous correction of ghost and geometric distortion artifacts in EPI using a multi-echo reference scan. *IEEE Trans Med Imaging* 2001;20:535–539. [PubMed: 11437113]
21. Neil JJ, Shiran SI, McKinstry RC, et al. Normal brain in human newborns: apparent diffusion coefficient and diffusion anisotropy measured by using diffusion tensor MR imaging. *Radiology* 1998;209:57–66. [PubMed: 9769812]
22. Papadakis NG, Xing D, Houston GC, et al. A study of rotationally invariant and symmetric indices of diffusion anisotropy. *Magn Reson Imaging* 1999;17:881–892. [PubMed: 10402595]
23. Baratti C, Barnett AS, Pierpaoli C. Comparative MR imaging study of brain maturation in kittens with T1, T2, and the trace of the diffusion tensor. *Radiology* 1999;210:133–142. [PubMed: 9885598]
24. Xiong J, Gao JH, Lancaster JL, Fox PT. Clustered pixels analysis for functional MRI activation studies of the human brain. *Hum Brain Mapp* 1995;3:287–301.
25. Rivkin MJ. Developmental neuroimaging of children using magnetic resonance techniques. *Ment Retard Dev Disabil Res Rev* 2000;6:68–80. [PubMed: 10899799]
26. Inder TE, Huppi PS. In vivo studies of brain development by magnetic resonance techniques. *Ment Retard Dev Disabil Res Rev* 2000;6:59–67. [PubMed: 10899798]
27. Mrzljak L, Uylings HB, Van Eden CG, Judas M. Neuronal development in human prefrontal cortex in prenatal and postnatal stages. *Prog Brain Res* 1990;85:185–222. [PubMed: 2094894]
28. Klingberg T, Vaidya CJ, Gabrieli JD, Moseley ME, Hedehus M. Myelination and organization of the frontal white matter in children: a diffusion tensor MRI study. *Neuroreport* 1999;10:2817–2821. [PubMed: 10511446]
29. Pierpaoli C, Jezzard P, Basser PJ, Barnett A, Di Chiro G. Diffusion tensor MR imaging of the human brain. *Radiology* 1996;201:637–648. [PubMed: 8939209]
30. Paus T, Zijdenbos A, Worsley K, et al. Structural maturation of neural pathways in children and adolescents: in vivo study. *Science* 1999;283:1908–1911. [PubMed: 10082463]
31. Shimony JS, McKinstry RC, Akbudak E, et al. Quantitative diffusion-tensor anisotropy brain MR imaging: normative human data and anatomic analysis. *Radiology* 1999;212:770–784. [PubMed: 10478246]

32. Giedd JN, Snell JW, Lange N, et al. Quantitative magnetic resonance imaging of human brain development: ages 4–18. *Cereb Cortex* 1996;6:551–560. [PubMed: 8670681]
33. Curnes JT, Burger PC, Djang WT, Boyko OB. MR imaging of compact white matter pathways. *AJNR Am J Neuroradiol* 1988;9:1061–1068. [PubMed: 3143230]
34. Muzik O, Chugani DC, Juhasz C, Shen C, Chugani HT. Statistical parametric mapping: assessment of application in children. *Neuroimage* 2000;12:538–549. [PubMed: 11034861]
35. Holland SK, Plante E, Byars AW, Straws-burg RH, Schmithorst VJ, Ball WS Jr. Normal fMRI brain activation patterns in children performing a verb generation task. *Neuroimage* 2001;14:837–843. [PubMed: 11554802]
36. Tanner SF, Ramenghi LA, Ridgway JP, et al. Quantitative comparison of intrabrain diffusion in adults and preterm and term neonates and infants. *AJR Am J Roentgenol* 2000;174:1643–1649. [PubMed: 10845500]
37. Wimberger DM, Roberts TP, Barkovich AJ, Prayer LM, Moseley ME, Kucharczyk J. Identification of “premyelination” by diffusion-weighted MRI. *J Comput Assist Tomogr* 1995;19:28–33. [PubMed: 7529780]
38. Beaulieu C, Allen PS. Determinants of anisotropic water diffusion in nerves. *Magn Reson Med* 1994;31:394–400. [PubMed: 8208115]
39. Virta A, Barnett A, Pierpaoli C. Visualizing and characterizing white matter fiber structure and architecture in the human pyramidal tract using diffusion tensor MRI. *Magn Reson Imaging* 1999;17:1121–1133. [PubMed: 10499674]
40. Kreis R, Ernst T, Ross BD. Development of the human brain: in vivo quantification of metabolite and water content with proton magnetic resonance spectroscopy. *Magn Reson Med* 1993;30:424–437. [PubMed: 8255190]
41. Lam WW, Wang ZJ, Zhao H, et al. 1H MR spectroscopy of the basal ganglia in childhood: a semiquantitative analysis. *Neuroradiology* 1998;40:315–323. [PubMed: 9638674]
42. Sadahiro S, Yoshikawa H, Yagi N, et al. Morphometric analysis of the myelin-associated oligodendrocytic basic protein-deficient mouse reveals a possible role for myelin-associated oligodendrocytic basic protein in regulating axonal diameter. *Neuroscience* 2000;98:361–367. [PubMed: 10854769]
43. Eyre JA, Miller S, Ramesh V. Constancy of central conduction delays during development in man: investigation of motor and somatosensory pathways. *J Physiol* 1991;434:441–452. [PubMed: 2023125]
44. Nezu A, Kimura S, Uehara S, Kobayashi T, Tanaka M, Saito K. Magnetic stimulation of motor cortex in children: maturity of corticospinal pathway and problem of clinical application. *Brain Dev* 1997;19:176–180. [PubMed: 9134188]
45. Butt AM, Berry M. Oligodendrocytes and the control of myelination in vivo: new insights from the rat anterior medullary velum. *J Neurosci Res* 2000;59:477–488. [PubMed: 10679786]
46. Takahashi M, Ono J, Harada K, Maeda M, Hackney DB. Diffusional anisotropy in cranial nerves with maturation: quantitative evaluation with diffusion MR imaging in rats. *Radiology* 2000;216:881–885. [PubMed: 10966726]
47. van der Toorn A, Sykova E, Dijkhuizen RM, et al. Dynamic changes in water ADC, energy metabolism, extracellular space volume, and tortuosity in neonatal rat brain during global ischemia. *Magn Reson Med* 1996;36:52–60. [PubMed: 8795020]

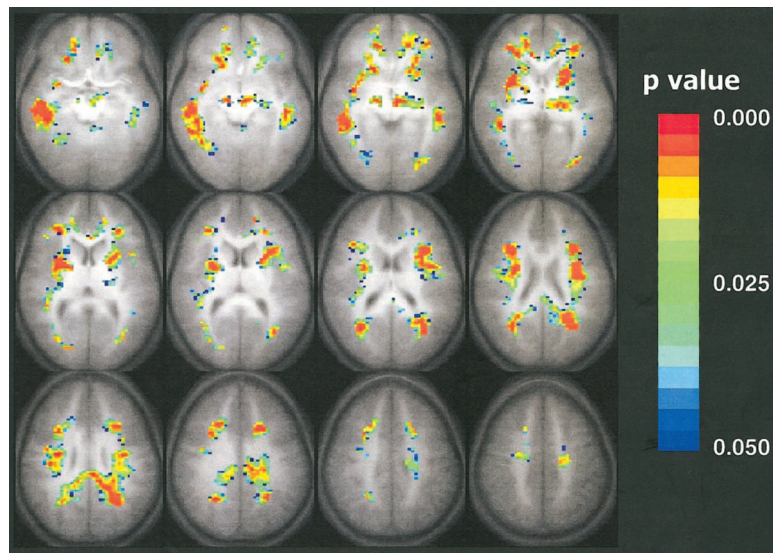


Figure 1.

Composite map of the trace of the apparent diffusion coefficient negatively correlated with respect to the age of the subject. Colored pixels have P values less than .05 according to the Spearman rank correlation test, with a cluster size of 15, and are overlaid on the average ($n = 33$) T1-weighted transverse whole-brain data set. The colors indicate the level of statistical significance from a P value less than .05 (blue) to a P value less than .003 (red). Statistically significant decreases in the trace of the apparent diffusion coefficient with age are shown throughout the white matter. Single-shot spin-echo echo-planar diffusion-tensor MR imaging parameters were as follows: 3,250/80; matrix, 64×128 ; field of view, 19.2×25.6 cm; section thickness, 5 mm; Δ , 40 msec; δ , 15 msec. Modified driven-equilibrium Fourier transform whole-brain anatomic imaging parameters were as follows: 18/4.3; matrix, $256 \times 128 \times 96$; field of view, $19.2 \times 25.6 \times 14.4$ cm; τ , 550 msec.

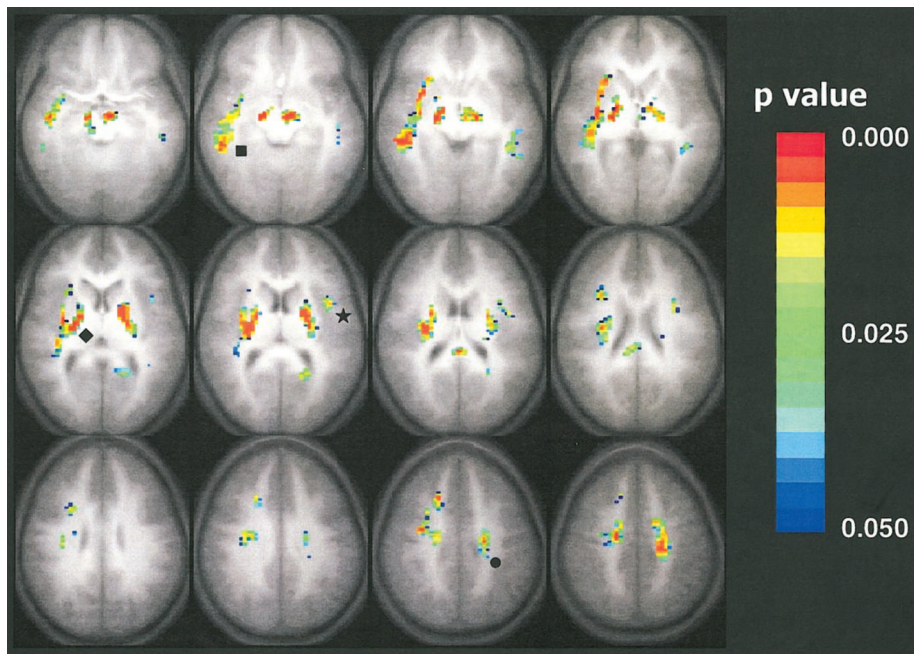


Figure 2.

Composite map of fractional anisotropy positively correlated with respect to the age of the subject. Colored pixels have P values less than .05 according to the Spearman rank correlation test, with a cluster size of 15, and are overlaid on the average ($n = 33$) T1-weighted transverse whole-brain data set. The colors indicate the level of statistical significance from a P value less than .05 (blue) to a P value less than .003 (red). Statistically significant increases in fractional anisotropy with age are shown in the internal capsule (◆), the corticospinal tract (●), the left arcuate fasciculus (★), and the right inferior longitudinal fasciculus (■). Single-shot spin-echo echo-planar diffusion-tensor MR imaging parameters were as follows: 3,250/80; matrix, 64×128 ; field of view, 19.2×25.6 cm; section thickness, 5 mm; Δ , 40 msec; δ , 15 msec. Modified driven-equilibrium Fourier transform whole-brain anatomic imaging parameters were as follows: 18/4.3; matrix, $256 \times 128 \times 96$; field of view, $19.2 \times 25.6 \times 14.4$ cm; τ , 550 msec.

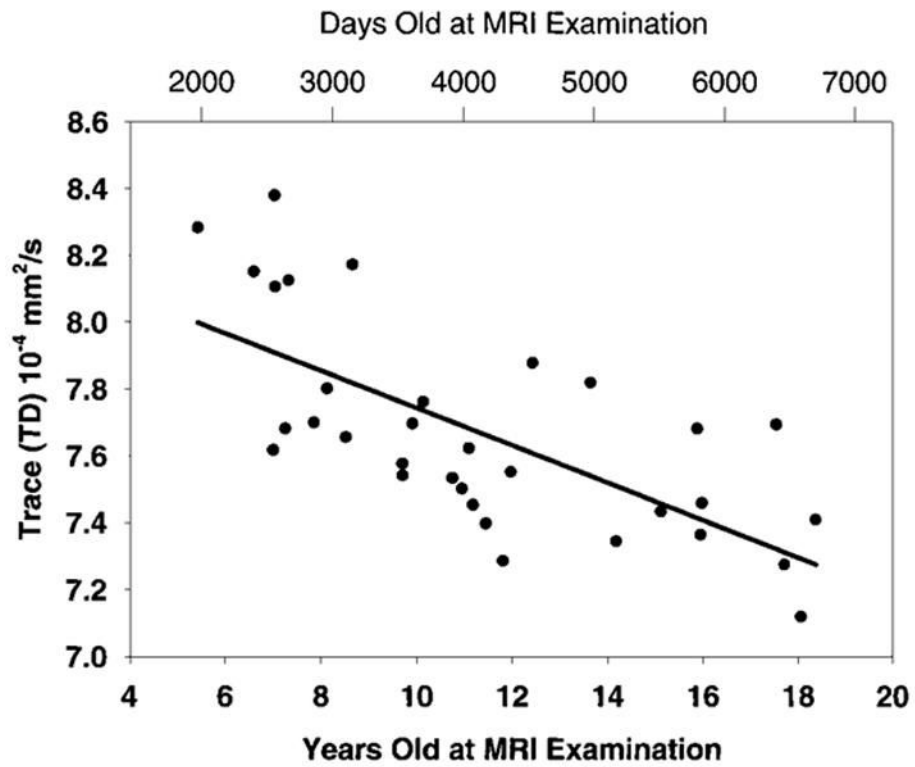


Figure 3. Scatterplot shows correlation of the trace of the apparent diffusion coefficient with age. The Spearman rank correlation coefficient, R , was -0.68 , and the P value was less than $.001$ for all pixels having a significant correlation in the sixth section (middle row, second image from left) of Figure 1.

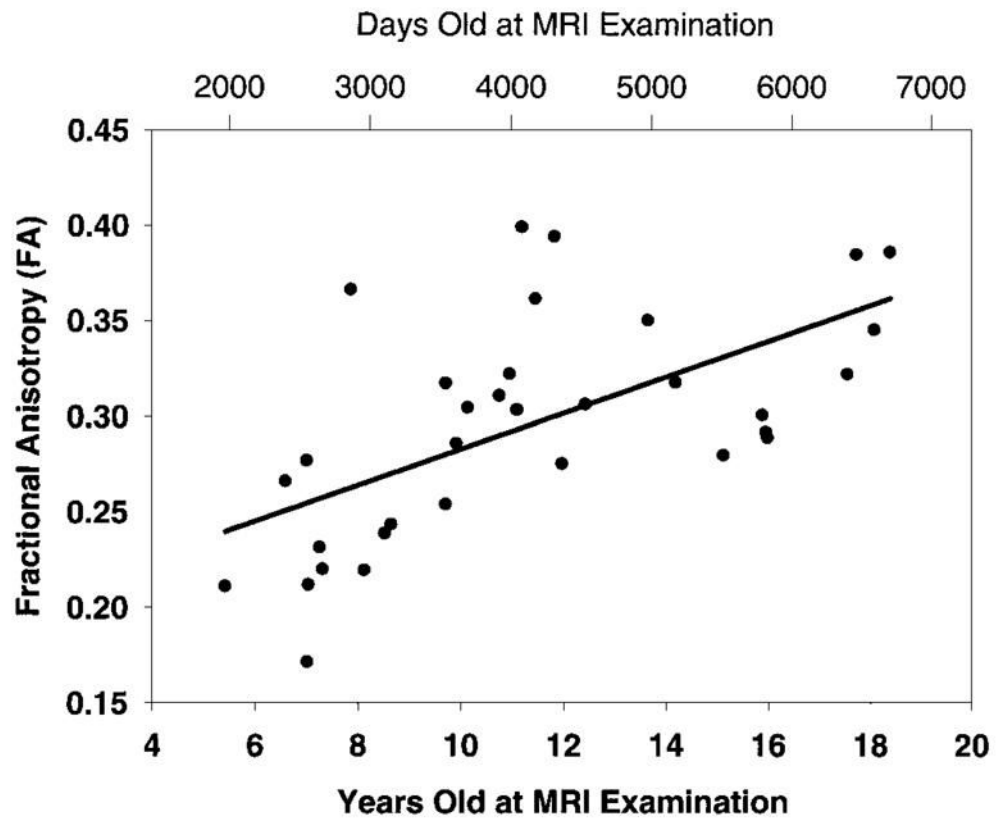


Figure 4. Scatterplot shows correlation of fractional anisotropy with age. The Spearman rank correlation coefficient, R , was 0.65, and the P value was less than .001 for all pixels having significant correlation in the sixth section (middle row, second image from left) of Figure 2.

Table

Number of Subjects according to Age and Sex

	Age (y)													
	5	6	7	8	9	10	11	12	13	14	15	16	17	18
Sex														
M	1	0	2	2	1	3	2	1	0	1	1	0	2	0
F	0	1	4	1	2	0	3	0	1	0	3	0	0	2